Spin-dependent Breit–Wigner and Fano resonances in photon-assisted electron transport through a semiconductor heterostructure*

Hu Li-Yun(胡丽云) and Zhou Bin(周 斌)†

Department of Physics, Hubei University, Wuhan 430062, *China*

(Received 10 August 2010; revised manuscript received 25 February 2011)

We theoretically investigate the electron transmission through a seven-layer semiconductor heterostructure with the Dresselhaus spin–orbit coupling under two applied oscillating fields. Numerical results show that both of the spin-dependent symmetric Breit–Wigner and the asymmetric Fano resonances appear and that the properties of these two types of resonance peaks are dependent on the amplitude and the relative phases of the two applied oscillating fields. The modulation of the spin-polarization efficiency of transmitted electrons by the relative phase is also discussed.

Keywords: spin–orbit coupling, Breit–Wigner resonance, Fano resonance

PACS: 72.25.Dc, 71.70.Ej, 85.75.Mm **DOI:** 10.1088/1674-1056/20/6/067201

1. Introduction

The spin-dependent tunneling of electrons in nonmagnetic semiconductor nanostructures is an interesting problem in the field of spintronics, in which the spin–orbit coupling (SOC) effect plays an important role. The SOC, which relates the electron spin to its momentum, may provide a controllable way to orient, manipulate and detect spins in semiconductors by electrical means. Structure inversion asymmetry in semiconductor heterojunctions, which may be induced either by growing an asymmetric structure or by the use of external electric field and leads to spin splitting of the conduction band in the momentum $\boldsymbol{k}$ space, induces so-called Rashba SOC.[1] This type of system may be a good candidate to implement spin-based electronic devices and has attracted more and more attention; moreover it is also noted that Rashba SOC in differential types of semiconductor quantum wells may show differential behaviors.[2,3] Since Voskoboynikov *et al.* indicated the possibility of creating a spin filter on the basis of tunneling through an asymmetric barrier in nonmagnetic semiconductors with Rashba SOC,[4,5] the dependence of the tunneling transmission probability on the electron–spin polarization in asymmetric semiconductor heterostructures with Rashba SOC has been extensively investigated.[6−11] For instance, a prototype side-gated asymmetric resonant interband tunneling device fabricated with an AlSb/InAs/GaSb/AlSb heterostructure for Rashba spin filter applications was proposed by Moon *et al.*[11] On the other hand, Perel' *et al.*[12] developed a theoretical model of a spin injector to show another mechanism of SOC, induced by a bulk inversion asymmetry and often referred to as Dresselhaus SOC,[13] can modify the effective mass of electron and lead to spin-dependent tunneling through a symmetric nonmagnetic semiconductor barrier. Since then, many efforts have been devoted to the study of the effect of the Dresselhaus SOC on electrons tunneling through the semiconductor heterostructures with or without an external electric field.[14−27] Moreover, the interplay between the Rashba and the Dresselhaus SOCs has also attracted considerable attention.[28−32]

When considering quantum transport in periodically driven semiconductor heterostructures, quantum interference between a bound state and the continuum of band leads to the appearance of asymmetric Fano-type resonance.[33,34] Recently, Zhang *et al.*[19] investigated the spin-dependent electron transmission through a quantum well with Dresselhaus SOC driven by a homogeneous oscillating field and indicated that Fano-type resonance can split into two asymmet-

*Project supported by the National Natural Science Foundation of China (Grant No. 10974046), Natural Science Foundation of Hubei Province of China (Grant No. 2009CDB360), and the Key Project of Education Department of Hubei Province of China (Grant No. D20101004).

†Corresponding author. E-mail: binzhou@hubu.edu.cn

© 2011 Chinese Physical Society and IOP Publishing Ltd

ric resonance peaks due to Dresselhaus SOC. Later on, the photon-mediated electron resonance transmission through a symmetric nonmagnetic semiconductor double-well structure with Dresselhaus SOC and two spatially homogeneous oscillating fields having a relative phase difference between them was also investigated.[24,26] It was demonstrated that the spin-dependent resonance peaks can be controlled by adjusting the relative phase difference between the two applied oscillating fields. In the present work, we will consider a seven-layer semiconductor heterostructure with Dresselhaus SOC and assume that the two spatially homogeneous applied oscillating fields are confined in quantum-well regions. The main characteristic of the structure considered here is that both of the symmetric Breit–Wigner resonances and asymmetric Fano resonances occur simultaneously. We will focus on the dependence of these two types of spin-dependent resonances on the amplitude and the relative phase of the two applied oscillating fields and present some fascinating features which can be used to design a tunable spin filter and to realize the modulation of spin.

2. Model and method

In this paper, we consider the transmission of electron with the initial wave vector $\boldsymbol{k} = (\boldsymbol{k}_{\parallel}, k_z)$ along the $z \parallel [001]$ direction through a seven-layer semiconductor heterostructure with Dresselhaus SOC [see Fig. 1: regions I ($z < -b$), IV ($a \leq z < a + c$) and VII ($z \geq 2a + b + c$) being made of GaAs with the effective mass of the electron μ_1 and Dresselhaus SOC constant γ_1; regions II ($-b \leq z < 0$) and VI ($2a + c \leq z < 2a + b + c$) $Ga_{0.7}Al_{0.3}As$ with μ_2 and γ_2; regions III ($0 \leq z < a$) and V ($a + c \leq z < 2a + c$) of GaSb with μ_3 and γ_3; a is the width of the wells, b and c are the thicknesses of the barriers]. Here $\boldsymbol{k}_{\parallel}$ is the wave vector parallel to the plane of the wells and k_z is the wave vector component normal to the well plane along the direction of transmission. To investigate the modulation of spin-dependent electron transport induced by the external fields, we assume that two spatially homogeneously applied oscillating fields $V_1 \cos(\omega t + \alpha)$ and $V_2 \cos(\omega t + \beta)$ are confined in the two well regions III and V, where $V_{1(2)}$, ω and $\alpha(\beta)$ denote the amplitudes, frequency and phases of applied oscillating fields, respectively. We also define a relative phase φ $(= \beta - \alpha)$ of the two applied oscillating fields. We use a single-electron model and neglect the charging effect as well as imperfections,[34] thus

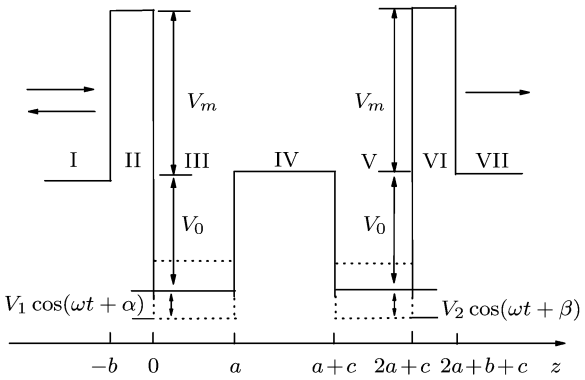


Fig. 1. Potential profile of a seven-layer semiconductor heterostructure with two spatially homogeneously applied oscillating fields. V_m is the height of the barriers and V_0 is the depth of the well; a is the width of the wells, b and c are the thicknesses of the barriers. $V_1 \cos(\omega t + \alpha)$ and $V_2 \cos(\omega t + \beta)$ are the two applied oscillating fields.

the Hamiltonian in each layer of the semiconductor structure may be given by

$$\hat{H} = -\frac{\hbar^2}{2\mu_i}\frac{\partial^2}{\partial z^2} + \frac{\hbar^2 k_{\parallel}^2}{2\mu_i} + V(z,t) + \hat{H}_{\mathrm{D}}, \qquad (1)$$

where $i = 1$, 2 and 3, $V(z,t)$ is a time-periodic potential [$V(z,t) = V(z,t+T)$ with $T = 2\pi/\omega$], and $\hat{H}_{\mathrm{D}}$ is the Dresselhaus SOC term. The potential profile of a harmonically driven heterostructure due to laser fields in the different regions is described by

$$V(z,t) = \begin{cases} 0, & \text{regions I, IV and VII;} \\ V_m, & \text{regions II and VI;} \\ -V_0 + V_1\cos(\omega t + \alpha), & \text{region III;} \\ -V_0 + V_2\cos(\omega t + \beta), & \text{region V;} \end{cases} \qquad (2)$$

the barrier height is V_m and the static well depth is V_0.

Assuming that the kinetic energy of incident electron is substantially smaller than the potential well depth V_0, then the Dresselhaus SOC term is simplified to[12]

$$\hat{H}_{\rm D} = \gamma_i \left(\hat{\sigma}_x k_x - \hat{\sigma}_y k_y\right) \frac{\partial^2}{\partial z^2}, \tag{3}$$

where $\hat{\sigma}_x$ and $\hat{\sigma}_y$ are the Pauli matrices. One can diagonalize the Dresselhaus SOC term $\hat{H}_{\rm D}$ by the spinors[15]

$$\chi_{\pm} = \frac{1}{\sqrt{2}} \begin{pmatrix} 1 \\ \mp {\rm e}^{-{\rm i}\,\phi} \end{pmatrix}, \tag{4}$$

which describe the electron spin states corresponding to the opposite spin directions, with + for the spin-up state and − for the spin-down state. Here ϕ is the polar angle of the wave vector $\boldsymbol{k}_{\parallel}$. Now we use the basis of the spin eigenstates ± to simplify the effective Hamiltonian $\hat{H}$ (1), thus the electron motion in each layer of the semiconductor structure may be described by a time-dependent Schrödinger equation

$${\rm i}\,\hbar \frac{\partial}{\partial t} \Phi_{\pm}(\boldsymbol{r}, t) = \hat{H}_{\pm} \Phi_{\pm}(\boldsymbol{r}, t), \tag{5}$$

where $\boldsymbol{r} = (x, y, z)$, $\Phi_{\pm}(\boldsymbol{r}, t) = \chi_{\pm} \psi_{\pm}(z, t) \exp\left({\rm i}\,\boldsymbol{k}_{\parallel} \cdot \boldsymbol{\rho}\right)$ with $\boldsymbol{\rho} = (x, y)$ being a vector parallel to the potential well plane and

$$\hat{H}_{\pm} = \chi_{\pm}^{\dagger} \hat{H} \chi_{\pm} = -\frac{\hbar^2}{2\mu_{i\pm}} \frac{\partial^2}{\partial z^2} + \frac{\hbar^2 k_{\parallel}^2}{2\mu_i} + V(z, t) \tag{6}$$

with $\mu_{i\pm} = \mu_i \left(1 \pm 2\gamma_i \mu_i k_{\parallel}/\hbar^2\right)^{-1}$ being the modified effective mass of electron. It is shown that the modified effective mass of electron $\mu_{i\pm}$ is not only associated with the Dresselhaus SOC constant and the in-plane wave vector, but also with the orientation of electron spin. One notes that in equilibrium the momentum distribution of the incident electrons is isotropic in the xy plane and therefore the average spin of the transmitted electrons vanishes.[15,21] Thus we assume that the in-plane wave vector of the incident electron is along a fixed direction to obtain the net spin polarization in the transmitted electrons.[21]

Since $V(z, t)$ is a time-periodic potential function in the Hamiltonian (6), the wavefunctions in the regions III and V can be expressed according to the Floquet theorem.[35–37] Moreover incident electrons will be scattered inelastically into an infinite number of Floquet sidebands inside the regions III and V, so the wavefunctions in the other regions can be written as the superposition of waves with all values of energy. The wavefunctions in seven semiconductor layers have the following forms, respectively,

$$\Phi_{\pm}^{\rm I} = \sum_{n=-\infty}^{+\infty} \eta \left(\delta_{n0}^{\pm} {\rm e}^{{\rm i}\,k_{zn}^{a\pm} z} + r_{n0}^{\pm} {\rm e}^{-{\rm i}\,k_{zn}^{a\pm} z}\right), \tag{7}$$

$$\Phi_{\pm}^{\rm II} = \sum_{n=-\infty}^{+\infty} \eta \left(c_{n1}^{\pm} {\rm e}^{-k_{zn}^{b\pm} z} + d_{n1}^{\pm} {\rm e}^{k_{zn}^{b\pm} z}\right), \tag{8}$$

$$\Phi_{\pm}^{\rm III} = \sum_{n=-\infty}^{+\infty} \sum_{m=-\infty}^{+\infty} \eta \left(a_{m1}^{\pm} {\rm e}^{{\rm i}\,q_m^{\pm} z} + b_{m1}^{\pm} {\rm e}^{-{\rm i}\,q_m^{\pm} z}\right) \times {\rm J}_{n-m}\left(\frac{V_1}{\hbar\omega}\right) \exp\left({\rm i}\,\frac{V_1}{\hbar\omega} \sin\alpha\right) {\rm e}^{-{\rm i}(n-m)\alpha}, \tag{9}$$

$$\Phi_{\pm}^{\rm IV} = \sum_{n=-\infty}^{+\infty} \eta \left(e_{n0}^{\pm} {\rm e}^{{\rm i}\,k_{zn}^{a\pm} z} + f_{n0}^{\pm} {\rm e}^{-{\rm i}\,k_{zn}^{a\pm} z}\right), \tag{10}$$

$$\Phi_{\pm}^{\rm V} = \sum_{n=-\infty}^{+\infty} \sum_{m=-\infty}^{+\infty} \eta \left(a_{m2}^{\pm} {\rm e}^{{\rm i}\,q_m^{\pm} z} + b_{m2}^{\pm} {\rm e}^{-iq_m^{\pm} z}\right) \times {\rm J}_{n-m}\left(\frac{V_2}{\hbar\omega}\right) \exp\left({\rm i}\,\frac{V_2}{\hbar\omega} \sin\beta\right) {\rm e}^{-{\rm i}(n-m)\beta}, \tag{11}$$

$$\Phi_{\pm}^{\rm VI} = \sum_{n=-\infty}^{+\infty} \eta \left(c_{n2}^{\pm} {\rm e}^{-k_{zn}^{b\pm} z} + d_{n2}^{\pm} {\rm e}^{k_{zn}^{b\pm} z}\right), \tag{12}$$

$$\Phi_{\pm}^{\rm VII} = \sum_{n=-\infty}^{+\infty} \eta t_{n0}^{\pm} {\rm e}^{{\rm i}\,k_{zn}^{a\pm} z}. \tag{13}$$

Here

$$\eta = \chi_{\pm} {\rm e}^{{\rm i}\,\boldsymbol{k}_{\parallel} \cdot \boldsymbol{\rho} - {\rm i}\,E_{\parallel}^{\pm} t/\hbar} {\rm e}^{-{\rm i}\,E_{zn}^{\pm} t/\hbar},$$
$$E_{\parallel}^{\pm} = \hbar^2 k_{\parallel}^2 / 2\mu_1,$$

${\rm J}_n(x)$ is the Bessel function of the first kind,

$$k_{zn}^{a\pm} = \left[\frac{2\mu_{1\pm}}{\hbar^2}\left(E_{z0}^{\pm} + n\hbar\omega\right)\right]^{1/2}, \tag{14}$$

$$k_{zn}^{b\pm} = \left[\frac{2\mu_{2\pm}}{\hbar^2}\left(V_m - E_{z0}^{\pm} - n\hbar\omega - \frac{\hbar^2 k_{\parallel}^2}{2\mu_1} + \frac{\hbar^2 k_{\parallel}^2}{2\mu_2}\right)\right]^{1/2}, \tag{15}$$

and

$$q_m^{\pm} = \left[\frac{2\mu_{3\pm}}{\hbar^2}\left(E_F^{\pm} + m\hbar\omega - \frac{\hbar^2 k_{\parallel}^2}{2\mu_3} + V_0\right)\right]^{1/2}, \tag{16}$$

where m is an integer and $E_F^{\pm}$ is the Floquet energy eigenvalue ($E_n^{\pm} = E_{zn}^{\pm} + E_{\parallel}^{\pm} = E_F^{\pm} + n\hbar\omega$ with n being the sideband index[33,38]). Based on the continuities of $\Phi_{\pm}$ and $\mu_{i\pm}^{-1} \cdot \partial\Phi_{\pm}/\partial z$ at the interfaces $z = -b$, $z = 0$, $z = a$, $z = a + c$, $z = 2a + c$, and $z = 2a + b + c$, the coefficients of the wavefunctions ($a_{m1(2)}^{\pm}$, $b_{m1(2)}^{\pm}$, $\delta_{n0}^{\pm}$, $r_{n0}^{\pm}$, $c_{n1(2)}^{\pm}$, $d_{n1(2)}^{\pm}$, $e_{n0}^{\pm}$, $f_{n0}^{\pm}$, and $t_{n0}^{\pm}$) can be solved numerically by making use of transfer matrix technique and constructing the Flouquet S matrix.[34,26] The coefficients $r_{n0}^{\pm}$ and $t_{n0}^{\pm}$ are the probability amplitudes of the reflecting waves and outgoing waves from the sideband 0 to sideband n, respectively. Thus, the total electron transmission probabilities of spin + and

spin − components are given by[21]

$$T^{\pm} = \sum_{n=0}^{+\infty} \frac{k_{zn}^{a\pm}}{k_{z0}^{a\pm}} \left| t_{n0}^{\pm} \right|^2 . \tag{17}$$

3. Results and discussions

We now investigate numerically the spin-dependent electron resonance transmission through this seven-layer semiconductor heterostructure. The minimum number of sidebands needed to be included in the sum of Eq. (17) is determined by the amplitude and the frequency of applied oscillating fields.[19,21] For the numerical calculations, we take the following parameters: $V_m = 250$ meV, $V_0 = 200$ meV, $k_{\|} = 0.2\ \mathrm{nm}^{-1}$, $\hbar\omega = 10$ meV, $a = 1.5$ nm, $b = 2.5$ nm, $c = 10$ nm, $\gamma_1 = 24\ \mathrm{meV{\cdot}nm^3}$, $\gamma_2 = 18\ \mathrm{meV{\cdot}nm^3}$, $\gamma_3 = 187\ \mathrm{meV{\cdot}nm^3}$, $\mu_1 = 0.067m_\mathrm{e}$, $\mu_2 = 0.092m_\mathrm{e}$, and $\mu_3 = 0.041m_\mathrm{e}$ with m_e being the mass of a free electron. It will be demonstrated that Dresselhaus SOC induces the splitting of the multiple spectrum and the line shapes of transmission resonances depend on the amplitude and the relative phase of oscillating fields.

In Fig. 2, we plot the transmission probability as a function of the incident electron energy for the different amplitudes of applied periodic oscillating fields with the relative phase $\varphi = 0$. Figure 2(a) shows the splitting of the resonance transmission in the absence of oscillating field (i.e., $V_1 = V_2 = 0$). The symmetric Breit–Wigner resonant peaks result from appearance of quasibound energy levels in the middle of the two higher barriers and incident energy $E_z^{\pm}$ equals the quasibound level $E_q^{\pm}$. The quasibound levels for spin-up and spin-down electrons are $E_q^{+} = 28.1$ meV and $E_q^{-} = 26.6$ meV, respectively. When two periodic oscillating fields are applied, the photon-assisted resonance transmission occurs because of the interaction between the incident electron and the oscillating fields, which results in the multiple structure of the transmission.[21,39] The positions of symmetric resonance peaks in Fig. 2 depend on the relation $E_z^{\pm} = E_q^{\pm} \pm n\hbar\omega$ and they are the process of photons emission or absorption. The lateral peaks in Figs. 2(b)–2(e) denote the one-photon absorption or emission process. Since the amplitudes of the oscillating fields determine the coupling strength between electron and the applied fields, the increase of the amplitudes of the fields will favour the probability of the one-photon process to occur. Thus, we can see clearly from Fig. 2 that with the increase of the amplitude of oscillating fields, the lateral peaks increase gradually while the symmetric Breit–Wigner resonant central peaks are suppressed. It is noted that the positions of the central peaks depend on the in-plane electron wave vector and have no relation to the oscillating fields; on the other hand, both the frequency of the applied oscillating fields and in-plane electron wave vector determined the positions of the lateral peaks. Therefore, the variation of the amplitude of oscillating fields cannot induce the shift of the positions of the symmetric Breit–Wigner resonant peaks. These properties of symmetric Breit–Wigner resonance are in agreement with the previous results.[21]

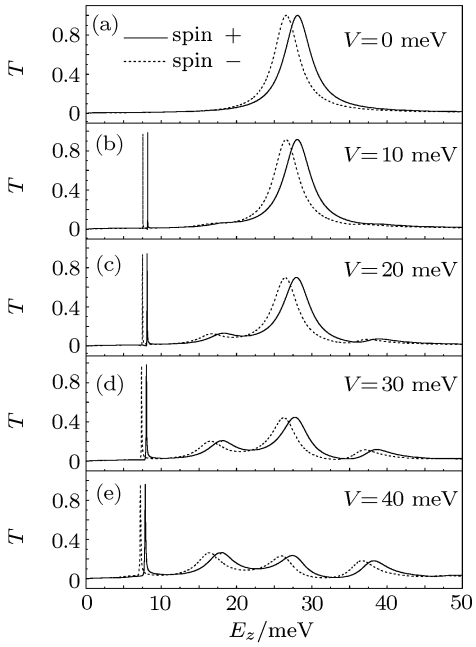


Fig. 2. The transmissivity of spin-up and spin-down electrons as a function of incident energy E_z for different amplitudes of oscillating fields with $V_1 = V_2 = V$, $V_m = 250$ meV, $V_0 = 200$ meV, $k_{\|} = 0.2\ \mathrm{nm}^{-1}$, $\hbar\omega = 10$ meV, $a = 1.5$ nm, $b = 2.5$ nm, $c = 10$ nm, $\mu_1 = 0.067m_\mathrm{e}$, $\mu_2 = 0.0092m_\mathrm{e}$, $\mu_3 = 0.041m_\mathrm{e}$, $\gamma_1 = 24\ \mathrm{meV{\cdot}nm^3}$, $\gamma_2 = 18\ \mathrm{meV{\cdot}nm^3}$, $\gamma_3 = 187\ \mathrm{meV{\cdot}nm^3}$, and $\alpha = \beta = 0$ (i.e., the relative phase $\varphi = 0$).

In Fig. 2, it is interesting to observe that the sharp asymmetric Fano-type resonant peaks appear on the left-hand side of Breit–Wigner resonant central peaks. Figure 2(b) shows that when $V_1 = V_2 = V = 10$ meV, the Fano resonance occurs at $E_z^{+} = 8.19$ meV for the spin + and $E_z^{-} = 7.57$ meV for the spin −. The corresponding bound-state energies are $E_b^{+} = -1.81$ meV, $E_b^{-} = -2.43$ meV, and resonance energies satisfy the relation $E_z^{\pm} = E_b^{\pm} + \hbar\omega$. The asymmetric Fano-type resonance arises from the interference between the discrete state and the continuum state.[40] In this seven-layer semiconductor heterostructure with two applied

oscillating fields ($V_1 = V_2 \neq 0$), the electron tunneling through the first barrier may emit a photon, dropping to the bound state bound level, and is then excited back to the original state by absorbing a photon to tunnel through the last barrier.[19,21] This photon-mediated tunneling process actually forms the discrete channel in the Fano-type resonance. If the energy of one (or multi-) photon is just consistent with the energy difference between the incident electrons and the bound states, the resonance transmission occurs. According to the Fano theory,[40,41] the Fano resonances of the transition probability have a line shape $\sim (\epsilon + q)^2 / (1 + \epsilon^2)$, with $\epsilon = (E - E_0) / (\Gamma/2)$, where E_0 and Γ are the energy position and width of the resonance state, respectively. The Fano's asymmetric parameter q is a measure of the coupling strength between the continuum state and the resonance state. For $q > 0$ ($q < 0$), a dip lies on the left-hand (right-hand) side of the asymmetric resonant peak.[24] In the limit of $q \to \infty$, the line shape of resonances evolves into a symmetric Breit–Wigner-type resonance.

Then, we plot the transmission probability as a function of the incident electron energy in a small energy scale corresponding to Fano resonance peaks in Fig. 3. The coupling strength between the electron and the applied oscillating fields depends on the amplitude of fields. This coupling effect leads to the broadening of the bound energy level and the asymmetric Fano resonance can take place within certain range of energy.[19] Thus, one can also observe that the widths of Fano-type resonance peaks broaden with increasing oscillation amplitude for both spin-up and spin-down electrons. On the other hand, the variation of the amplitudes of the two oscillating fields affects the coupling between two potential wells (regions III and V) and leads to the shift of the bound energy levels in two potential wells. Therefore, it is shown in Fig. 3 that both for spin + and spin − the asymmetric Fano resonance peaks move toward the direction of low energy as the amplitude of oscillating fields increases.

The shapes of the symmetric and asymmetric resonance peaks in energy parameter space depend not only on the amplitude of the external fields, but also on the relative phase of the external fields. The corresponding results for the phase modulation of transmission coefficients on the opposite spin orientation are presented in Figs. 4 and 5. In Fig. 4, we plot the transmission probability as a function of the incident electron energy with the variation of relative phase φ ($= \beta - \alpha$). It is noted from Eqs. (9) and (11) that the wavefunctions $\Phi_{\pm}^{\mathrm{III}}$ and $\Phi_{\pm}^{\mathrm{V}}$ in the potential wells have an additional phase relation to the phases of applied oscillating fields. When the two oscillating fields are applied in regions III and V, the relative phase φ between the two oscillating fields may weaken the probability of one-photon process and enhance the direct resonance transmission. As a result, it is shown in Fig. 4 that when the relative phase of the two oscillating fields changes from 0 to π, the symmetric

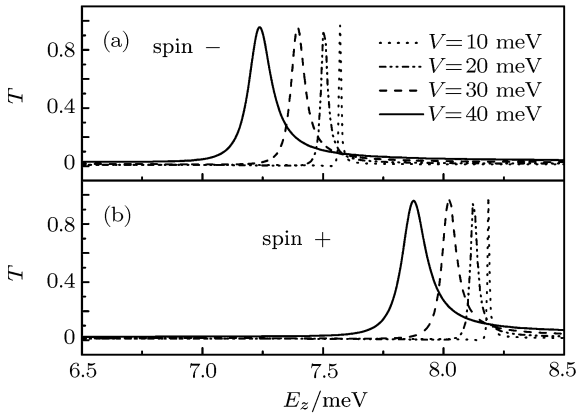


Fig. 3. The transmissivity versus E_z in a small energy scale for different amplitudes of oscillating fields. The parameters are given in Fig. 2 (with relative phase $\varphi = 0$), (a) for spin + and (b) for spin −.

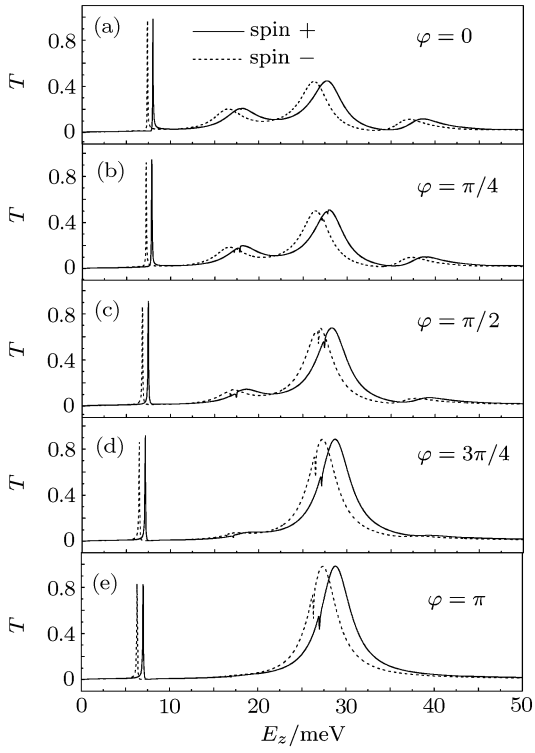


Fig. 4. The transmissivity versus E_z for different relative phases between oscillating fields with $V_1 = V_2 = 30$ meV. The other parameters are the same as those in Fig. 2.

Breit–Wigner resonant central peaks increase gradually while the lateral peaks are suppressed and almost disappear at $\varphi = \pi$. Moreover, the relative phase φ directly modifies the quasibound energy levels in the middle of two higher barriers, thus the position of the symmetric resonance moves gradually toward the direction of high energy. These phenomena imply that the relative phase influences the position and the amplitude of the symmetric Breit–Wigner resonance peaks. Additionally, figure 4(c) shows three sets of Fano resonance peaks for spin-up and spin-down electrons. For instance, in the case of spin-up electrons the resonance energies are $E_z^+ = 7.50$ meV, 17.51 meV, and 27.51 meV. In fact, they are the multi-photon Fano resonance processes and the resonance energies satisfy the relation $E_z^{\pm} = E_b^{\pm} + n\hbar\omega$. Furthermore, the probabilities of two-photon and three-photon processes are much less than one-photon process, which is similar to the cases in Figs. 4(b), 4(d), and 4(e).

Now we focus again on the asymmetric Fano resonance peaks. When the system has the time-reversal symmetry, the Fano's asymmetric parameter q is conventionally considered to be real. However, if the time-reversal symmetry is broken, the asymmetric parameter q should be a complex number and the line shape of the resonances may be expressed as $\sim \left[(\epsilon + \mathrm{Re}\, q)^2 + (\mathrm{Im}\, q)^2\right] / \left(1 + \epsilon^2\right)$.[41,42] The line shape of the resonances is asymmetric and symmetric for $|\mathrm{Re}\, q| \gg |\mathrm{Im}\, q|$ and $|\mathrm{Re}\, q| \ll |\mathrm{Im}\, q|$, respectively. In the case of asymmetric line shapes, a dip lies on the left-hand (right-hand) side of the asymmetric resonant peak for $\mathrm{Re}\, q > 0$ ($\mathrm{Re}\, q < 0$).[24] In the system considered here, the different phases between two oscillating fields leads to the breaking of the time-reversal symmetry, thus the asymmetric parameter q and the line shape of the transmission resonance may be modified by the relative phase of the two oscillating fields. The shapes of asymmetric Fano resonance peaks depend on the relative phase of the external fields, which are plotted in Fig. 5. The variation of the relative phase of the two oscillating fields adjusts the tunneling of electron through the middle barrier (region IV) between two potential wells (regions III and V), which leads to the shift of the bound energy levels. Therefore, one can observe that when φ changes from 0 to π, the positions of Fano resonant peaks move toward the direction of low energy. In addition, the amplitude and the dip of the asymmetry resonance peaks also changes with the relative phase. For both of the spin-up and spin-down electron states, when φ changes from 0 to π, the amplitude decreases gradually and the dip of the asymmetry resonance shifts from left-hand side to right-hand side. Moreover, at a special value of the relative phase about $\varphi = 3\pi/8$, the transmission asymmetry resonance peaks degenerate to the symmetric peaks. According to the theory mentioned above, for the relative phase $\varphi \in (0, 3\pi/8)$, $\mathrm{Re}\, q$ of the asymmetric parameter q is larger than zero and for $\varphi \in (3\pi/8, \pi)$ $\mathrm{Re}\, q$ is less than zero. The special value of the relative phase φ ($= 3\pi/8$) actually corresponds to the limiting case of $\mathrm{Re}\, q \to 0$ (and $\mathrm{Im}\, q \neq 0$), thus the Fano asymmetric lineshapes disappear and the symmetric peaks occur.

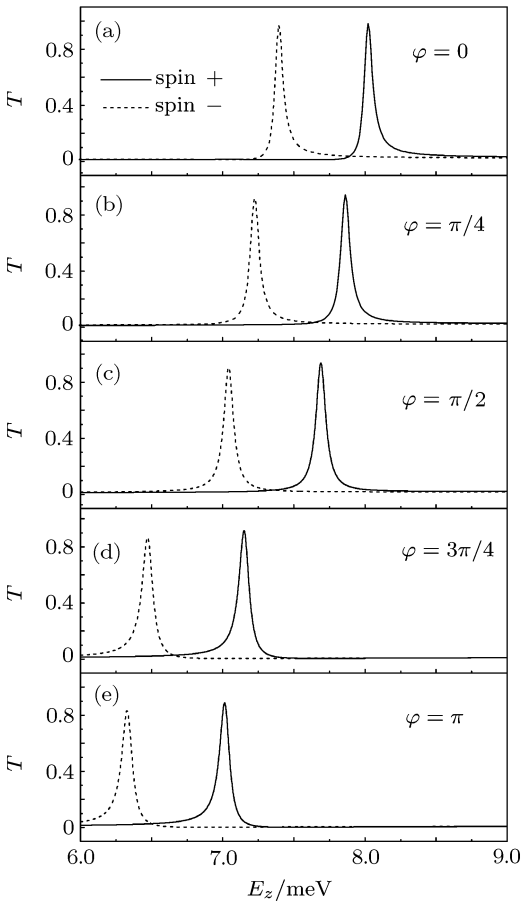


Fig. 5. The transmissivity versus E_z in a small energy scale for different relative phases of oscillating fields with $V_1 = V_2 = 30$ meV, and the other parameters are the same as those in Fig. 2.

The spin-dependent splitting of Fano-type resonance peaks plays an important role in realizing the spin polarization current. The spin polarization of electrons as a function of the relative phase φ is shown in Fig. 6 according to $P = (T^+ - T^-) / (T^+ + T^-)$ for the incident electron with energies $E_z = 8.02$ meV and 7.39 meV. When φ increases from 0 to 2π, for the case

of $E_z = 8.02$ meV, the spin-up polarization is dominant and it changes from about 0 to +0.9, but for the case of $E_z = 7.39$ meV, the spin polarization changes from −1.0 to +1.0. Thus we can design a tunable spin-polarization modulator and control the spin polarization of the current on the basis of the modulation of the relative phase of the two oscillating fields.

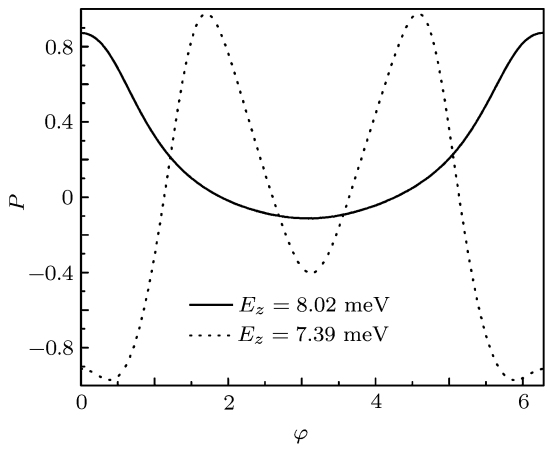


Fig. 6. The spin-polarization efficiency of the transmitted electrons as a function of relative phase for E_z = 8.02 meV, 7.39 meV, $V_1 = V_2 = 30$ meV and the other parameters are the same as those in Fig. 2.

4. Conclusions

In conclusion, we have investigated above the electron transmission through a seven-layer semiconductor heterostructure with Dresselhaus SOC and two applied oscillating fields. It is shown that SOC causes the spin splitting of the symmetric Breit–Wigner resonance peaks and the asymmetric Fano resonance peaks. Numerical results present that the amplitude and the relative phase of the two applied oscillation fields can influence the features of resonance peaks. As the amplitude of oscillating fields increases, the symmetric Breit–Wigner resonant central peaks are suppressed while the lateral peaks increase gradually and the asymmetric Fano resonance peaks move toward the direction of low energy and the width of peaks broadens. On the other hand, when the relative phase of oscillating fields changes from 0 to π, the symmetric Breit–Wigner resonant central peaks increase gradually but the lateral peaks are suppressed and the positions of the symmetric resonance peaks move toward direction of high energy, while the asymmetric resonance peaks move toward the direction of low energy. Moreover, for both the spin-up and spin-down states, the amplitude of Fano resonance peaks decreases gradually and the dip of asymmetry resonance shifts from left-hand side to right-hand side. Finally, the modulation of the spin-polarization efficiency of transmitted electrons by the relative phase was also discussed. These features can be applied to the design of a tunable spin filter and to realize the modulation of spin.

References

[1] Rashba E I 1960 *Sov. Phys. Solid State* **2** 1109

[2] Yang W and Chang K 2006 *Phys. Rev.* B **74** 193314

[3] Li J, Yang W and Chang K 2009 *Phys. Rev.* B **80** 035303

[4] Voskoboynikov A, Liu S S and Lee C P 1998 *Phys. Rev.* B **58** 15397

[5] Voskoboynikov A, Liu S S and Lee C P 1999 *Phys. Rev.* B **59** 12514

[6] de Andrada e Silva E A and La Rocca G C 1999 *Phys. Rev.* B **59** 15583

[7] Voskoboynikov A, Liu S S, Lee C P and Tretyak O 2000 *J. Appl. Phys.* **87** 387

[8] Araújo C M, da Silva A F and Silva E A D E 2002 *Phys. Rev.* B **65** 235305

[9] Ting D Z Y and Cartoixà X 2002 *Appl. Phys. Lett.* **81** 4198

[10] Koga T, Nitta J, Takayanagi H and Datta S 2002 *Phys. Rev. Lett.* **88** 126601

[11] Moon J S, Chow D H, Schulman J N, Deelman P, Zinck J J and Ting D Z Y 2004 *Appl. Phys. Lett.* **85** 678

[12] Perel' V I, Tarasenko S A, Yassievich I N, Ganichev S D, Bel'kov V V and Prettl W 2003 *Phys. Rev.* B **67** 201304(R)

[13] Dresselhaus G 1955 *Phys. Rev.* **100** 580

[14] Tarasenko S A, Perel' V I and Yassievich I N 2004 *Phys. Rev. Lett.* **93** 056601

[15] Glazov M M, Alekseev P S, Odnoblyudov M A, Chistyakov V M, Tarasenko S A and Yassievich I N 2005 *Phys. Rev.* B **71** 155313

[16] Yu L and Voskoboynikov O 2005 *J. Appl. Phys.* **98** 023716

[17] Wang L G, Yang W, Chang K and Chan K S 2005 *Phys. Rev.* B **72** 153314

[18] Li W and Guo Y 2006 *Phys. Rev.* B **73** 205311

[19] Zhang C X, Nie Y H and Liang J Q 2006 *Phys. Rev.* B **73** 085307

[20] Alekseev P S, Chistyakov V M and Yassievich I N 2006 *Semiconductors* **40** 1402

[21] Ye C Z, Zhang C X, Nie Y H and Liang J Q 2007 *Phys. Rev.* B **76** 035345

[22] Gong J, Liang X X and Ban S L 2007 *J. Appl. Phys.* **102** 073718

[23] Zhang C X, Wang R, Nie Y H and Liang J Q 2008 *Chin. Phys.* B **17** 2662

[24] Zhang C X, Nie Y H and Liang J Q 2008 *Chin. Phys.* B **17** 2670
[25] Nguyen T L H, Drouhin H J, Wegrowe J E and Fishman G 2009 *Phys. Rev.* B **79** 165204
[26] Xue H B, Nie Y H, Li Z J and Liang J Q 2010 *Physica* E **42** 1934
[27] Wan F, Jalil M B A and Tan S G 2009 *J. Appl. Phys.* **105** 07C704
[28] Yu L, Huang H C and Voskoboynikov O 2003 *Superlattice Microst.* **34** 547
[29] Gnanasekar K and Navaneethakrishnan K 2006 *Eur. Phys. J.* B **53** 455
[30] Isić G, Radovanović J and Milanović V 2007 *J. Appl. Phys.* **102** 123704
[31] Erić M, Radovanović J, Milanović V, Ikonić Z and Indjin D 2008 *J. Appl. Phys.* **103** 083701
[32] Fujita T, Jalil M B A and Tan S G 2008 *J. Phys.: Condens. Matter* **20** 115206
[33] Li W and Reichl L E 1999 *Phys. Rev.* B **60** 15732
[34] Li W and Reichl L E 2000 *Phys. Rev.* B **62** 8269
[35] Shirley J H 1965 *Phys. Rev.* **138** B979
[36] Holthaus M and Hone D 1993 *Phys. Rev.* B **47** 6499
[37] Fromherz T 1997 *Phys. Rev.* B **56** 4772
[38] Bagwell P F and Lake R K 1992 *Phys. Rev.* B **46** 15329
[39] del Valle C P, Lefebvre R and Atabek O 1999 *Phys. Rev.* A **59** 3701
[40] Fano U 1961 *Phys. Rev.* **124** 1866
[41] Kobayashi K, Aikawa H, Katsumoto S and Iye Y 2003 *Phys. Rev.* B **68** 235304
[42] Kobayashi K, Aikawa H, Katsumoto S and Iye Y 2002 *Phys. Rev. Lett.* **88** 256806